Journal of Superconductivity and Novel Magnetism (2018) 31:2925–2934
https://doi.org/10.1007/s10948-017-4539-x

ORIGINAL PAPER

Influence of Cation Size on the Electronic and Magnetic Structure of $MCoO_3$ (M = Bi, La) from Ab Initio Calculations

M. Djebari[1] · A. Zaoui[1] · M. Djermouni[1,2] · S. Kacimi[1] · N. Benayad[1]

Received: 18 October 2017 / Accepted: 21 December 2017 / Published online: 17 January 2018

Abstract

Using the first-principle DFT method and LSDA+U calculations, we have performed a detailed investigation on the structural and magnetic ground states of strongly correlated $MCoO_3$ (M = Bi, La) perovskites. Magneticphase stabilities, structural behaviors and electronic properties of both materials have been investigated. LSDA+U calculations show that the antiferromagnetic (AFM)-C phase in the tetragonal La/$BiCoO_3$ is energetically more favorable than the other configurations, and both rhombohedral materials are nonmagnetic. All structural data of tetragonal $BiCoO_3$ and rhombohedral $LaCoO_3$ compounds are found in excellent agreement with the experiment for U_{eff} = 6 eV. We have predicted also band gaps and magnetic moments with a good accuracy via the band structure calculations. From the total and partial densities of states, we have shown the important role of O pCo d and Bi/La s-O p hybridizations in both systems.

Keywords Density functional theory · LSDA+U · Electronic and magnetic structures · Perovskite materials

1 Introduction

A few multiferroic materials that possess both ferroelectricity and magnetism [1] are currently intensively investigated due to their potential technological applications in a variety of fields [2]. In multifunctional material technology, it is advantageous to have a high critical temperature and a high value of spontaneous polarization simultaneously. For this purpose, perovskite materials with general formula ABO_3 are extensively studied. The majority of known magnetic-ferroelectric perovskites contain Bi or Pb atoms at A-site which have a *lone pair* effect and a transition metal atom having unfilled d orbital at B-site [3]. A-cation leads to ferroelectricity while B-cation leads to magnetism [4]. Along the same line of thought, compounds like $BiFeO_3$ [5] and $PbVO_3$ [6] have been synthesized and they display a large spontaneous polarization as well as large critical temperatures simultaneously with antiferromagnetic spin ordering at the B-site [4]. Following this idea, multiferroic $BiCoO_3$ (BCO) has been carried out; BCO adopts a tetragonal $PbTiO_3$ structure type where the cobalt ion is coordinated by five oxygen ions which make a pyramidal polyhedron [7]. The pyramidal coordination for Co ion arises from the noncentrosymmetric position of Bi^{3+} atom [8]. The enclosed d^6 shell of Co^{3+} ion possesses three possibilities of spin configuration: low-spin (LS), intermediate-spin (IS), or high-spin (HS) configurations. $BiCoO_3$ is an insulator antiferromagnetic (AFM) below T_N = 470 K with antiferromagnetic in the ab-plane stacked ferromagnetically in the c-direction (AFM-C)-type spin order, where the spin magnetic moments of cobalt ions are antiferromagnetically aligned in xy-plane and are ferromagnetically stacked along the z-axis [8, 9].

At ambient conditions, $BiCoO_3$ has a tetragonal structure with a high tetragonality (1.27) associated with a large spontaneous polarization (170 $\mu C/cm^2$) [10] and a HS state-AFM-C spin ordering of cobalt ion [4]. Decreasing the temperature, it is found that the spin electron of Co^{3+} retains its HS state up to low temperature which prevents the spin-state transition as in the case of $LaCoO_3$ [11].

✉ A. Zaoui
ali_zaoui@yahoo.fr

[1] Laboratoire de Physique Computationnelle des Matériaux, Université Djillali Liabés de Sidi Bel-Abbés, Sidi Bel-Abbés 22000, Algérie

[2] Département de Physique, Institut de Sciences de la nature et de vie & Sciences exactes (SNV-SE), Centre Universitaire Ahmed ZABANA, Relizane, Relizane 48000, Algérie

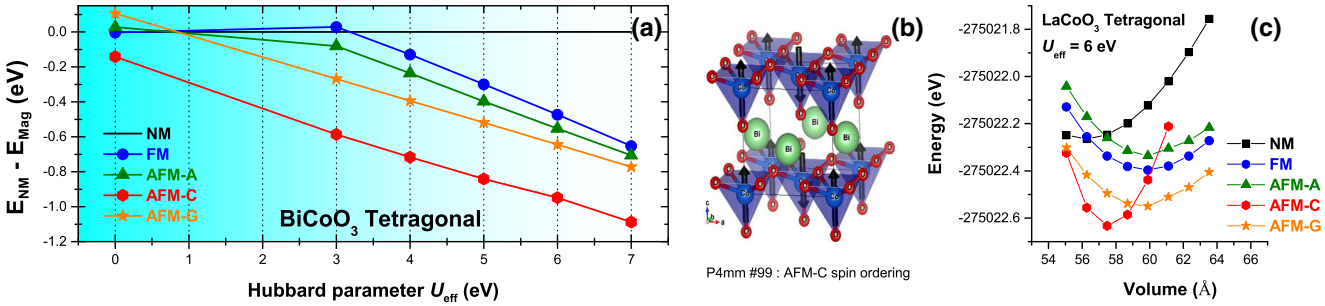

Fig. 1 Magnetic stability: **a** energies of various spin configurations of $BiCoO_3$ relative to the nonmagnetic case; **b** tetragonal AFM-C crystalstructure; and **c** variation of energies in various spin configurations of $LaCoO_3$ using LSDA+U (U = 6 eV)

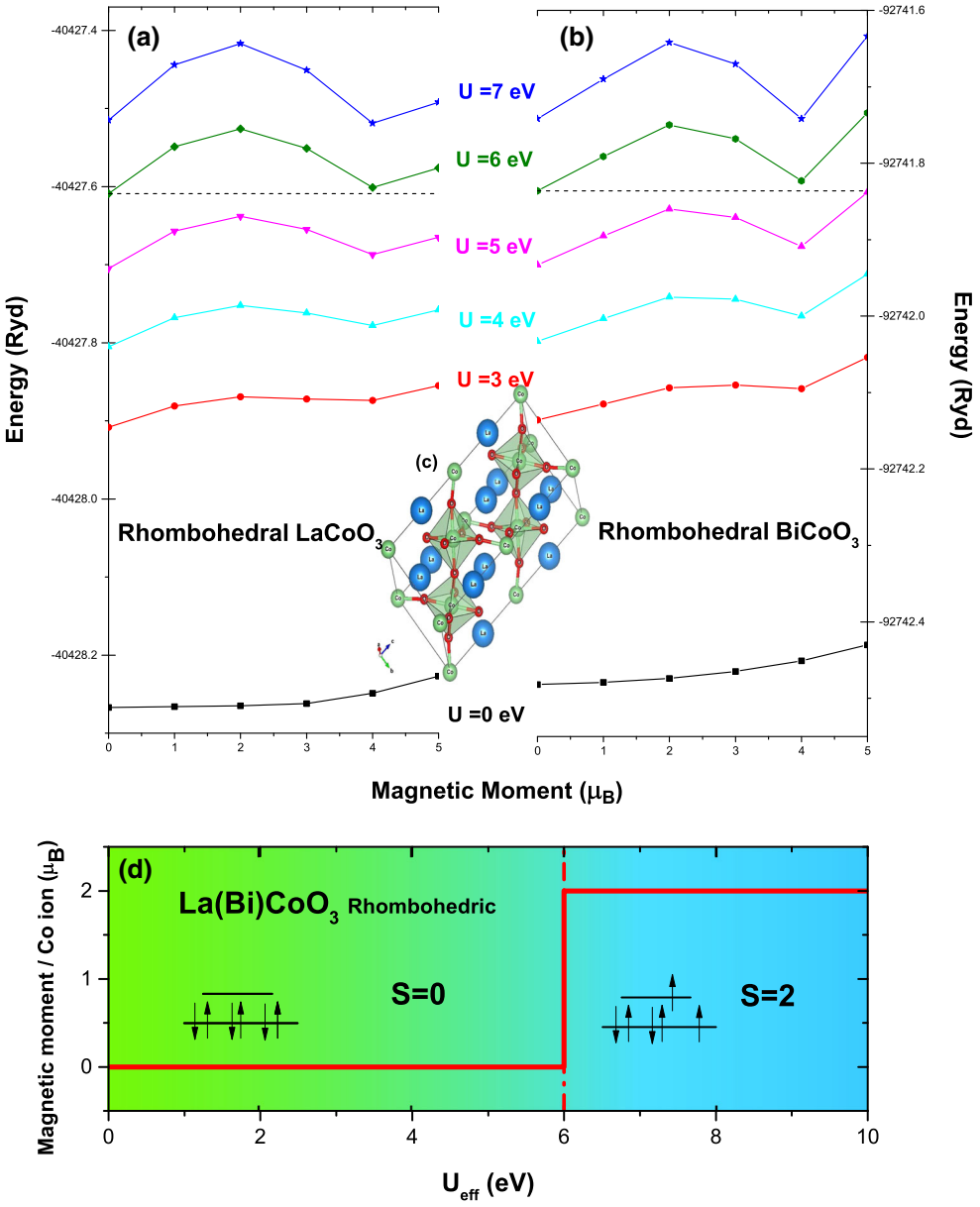

Fig. 2 FSM curves for $LaCoO_3$ (**a**) and $BiCoO_3$ (**b**) (U_{eff} = 0 to 7 eV) obtained by LSDA+U calculation **c** The rhombohedral unit cell **d** Variation of MM of Co-ion versus U_{eff} for $LaCoO_3$ and $BiCoO_3$

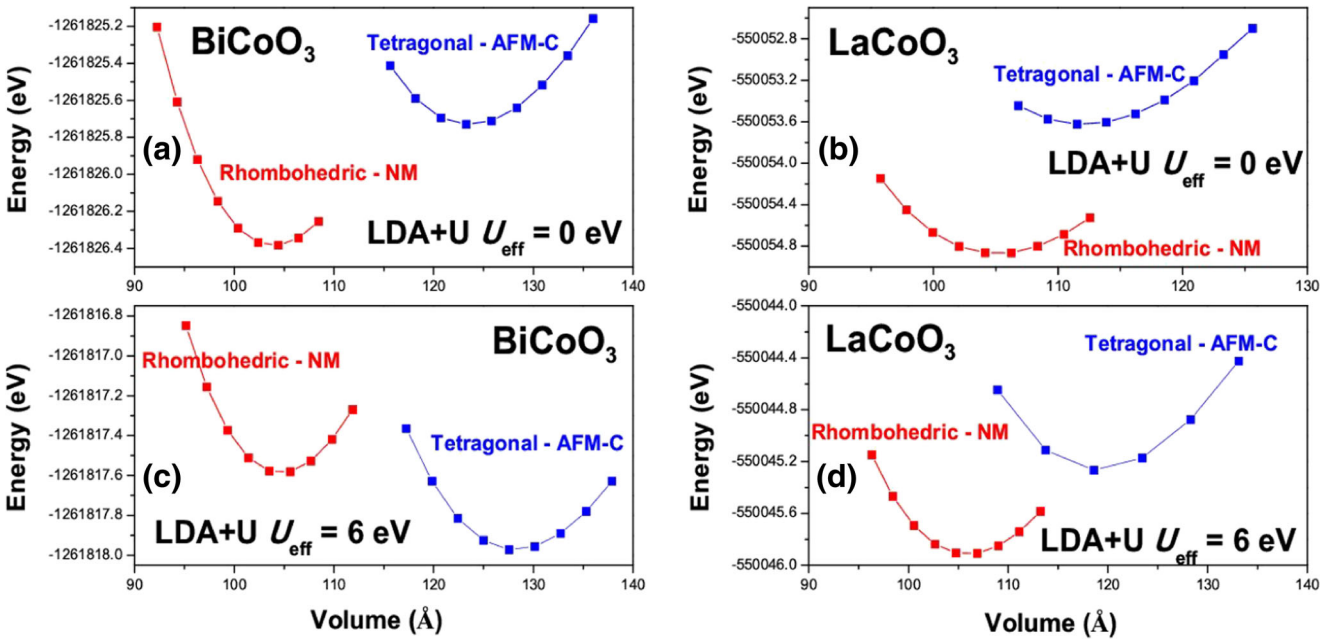

Fig. 3 Variation of total energies with LSDA+U (U = 0 and 6 eV)

Bi^{3+} and La^{3+} have a similar ionic radius; consequently, the local Co–O bond lengths in $BiCoO_3$ at high pressure-nonmagnetic (LS) phase is identical to those of $LaCoO_3$ in its ambient condition phase (LS state: Co–O = 1.925 Å at 5 K) [12, 13].

The A-site chemical modification of the ABO_3 structure is expected to affect the ferroelectric (FE) properties. Kan et al. [14] have shown that an enhanced dielectric response is obtained in $BiFeO_3$ compounds in which Bi is partially substituted by a rare-earth RE ions (RE = La, Sm, Gd, Dy, etc.).

In this article, we show the influence of cation size on the structural, electronic, and magnetic properties of $MCoO_3$ (M = Bi, La) in tetragonal and rhombohedral structures using local spin-density approximation (LSDA)+U calculations. We also discuss the bonding mechanism effects on magnetism and ferroelectricity phenomena in these systems.

2 Computational Methods

The calculations have been performed within density functional theory (DFT) implemented in the Wien2*k* package [15] based on the hybrid full-potential L/APW+*lo* method [16]. In this formalism, the unit cell is divided into two regions, nonoverlapping muffin-tin (MT) spheres, inside of which the basis functions are expanded in spherical harmonics and the basis functions in the interstitial

Table 1 Optimized lattice constants and atomic positions of tetragonal $BiCoO_3$ in AFM-C ordering compared with theoretical and experimental data (values set in italics are in good agreement with experimental data)

$BiCoO_3$T AFM-C	a (Å)	c (Å)	z_{Co}	Z_{O1}	Z_{O2}
FP-LAPW, LSDA+U, $U = 0$[a]	3.6008	*4.7663*	0.5723	0.1994	0.7088
FP-LAPW, LSDA+U, $U = 3$[a]	3.6385	4.7821	0.5681	0.2018	0.7186
FP-LAPW, LSDA+U, $U = 4$[a]	3.6422	4.7858	0.5681	0.2019	0.7196
FP-LAPW, LSDA+U, $U = 5$[a]	3.6462	4.7884	0.5680	*0.2016*	0.7208
FP-LAPW, LSDA+U, $U = 6$[a]	*3.6539*	4.8025	*0.5664*	*0.2052*	*0.7230*
FP-LAPW, LSDA+U, $U = 7$[a]	3.6480	4.7943	0.5675	0.2002	0.7201
PP [23]	3.7304	4.7897	0.5718	0.2015	0.7194
FP-LAPW, LSDA+U [25]	3.748	4.710	0.5658	0.2053	0.7287
FP-LAPW, LSDA [24]	3.73055	4.72613	0.57382	0.21421	0.72207
Experiment [23]	3.7199	4.7196	0.5664	0.2024	0.7311
Experiment [21]	3.729	4.723	0.5669	0.2034	0.7300

[a]Present calculation

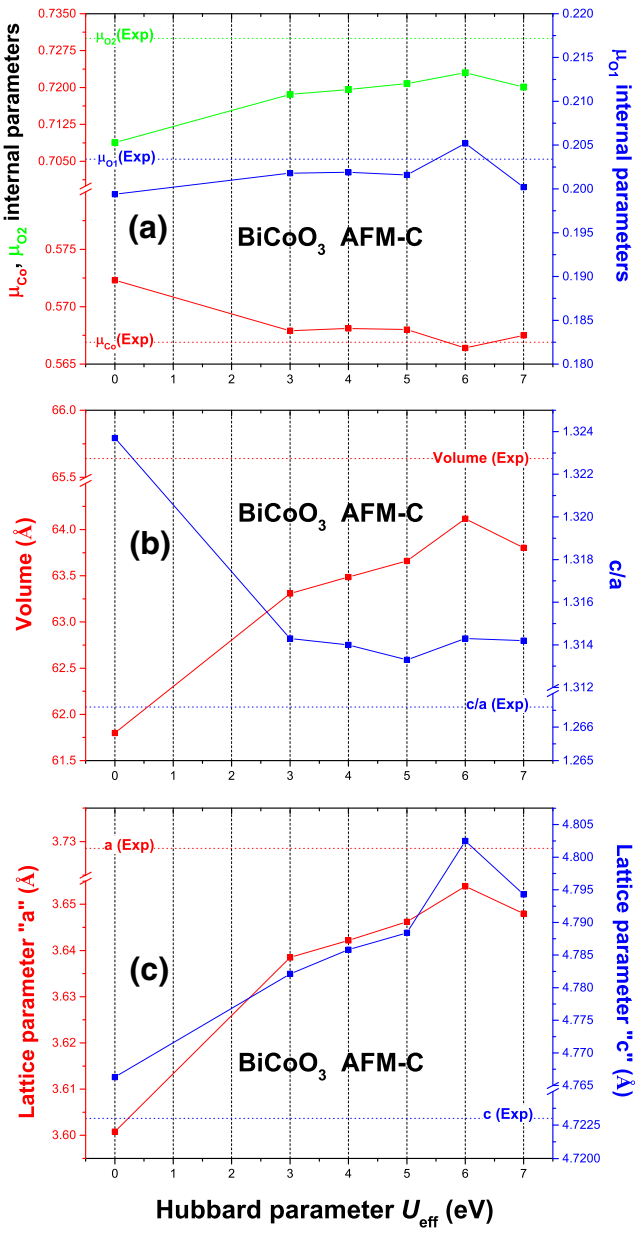

Fig. 4 **a** Variation of z_{Co}, z_{O1}, and z_{O2} versus U_{eff} **b** Variation of volume and c/a versus U_{eff} **c** Variation of a and c versus U_{eff} for $BiCoO_3$

region, outside the MT spheres, are plane waves. For the exchange-correlation potential, we employed a local-density approximation (LDA) built from the Perdew-Wang parametrization [17]. In order to describe the behavior of the localized Co d electrons, we have included the orbital-dependent, on-site Coulomb potential (Hubbard U) in the calculation within the so-called LSDA+U method [18]. Energy convergence in terms of the number of k-points has also been achieved. The bulk moduli and the equilibrium lattice parameters were evaluated using the Murnaghan equation of state [19] to fit the volume-energy curves. The

Table 2 Optimized lattice constants and atomic positions of rhombohedral $LaCoO_3$ in NM state compared with theoretical and experimental data (values set in italics are in good agreement with experimental data)

$LaCoO_3$R NM	a (Å)	α (deg)	x_O
LDA+U, $U = 0$[a]	5.242	61.4226	0.19799
LDA+U, $U = 3$[a]	5.2552	61.2266	0.19647
LDA+U, $U = 4$[a]	5.2585	61.1533	0.19718
LDA+U, $U = 5$[a]	5.2641	61.0826	0.19787
LDA+U, $U = 6$[a]	5.2683	61.0761	0.19792
LDA+U, $U = 7$[a]	5.2777	60.9141	0.19860
LDA+U [28]	5.4208	61.1287	–
U_{sc} [29]	5.3374	61.14	–
LDA	5.3283	61.4	–
Experiment [12]	5.297	61.01	0.19735
Experiment [13]	5.3416	60.99	0.1978

[a]Present calculation

electronic states of atoms in the crystal were chosen with the valence configurations of Bi: $5d^{10}\ 6s^2\ 6p^3$, La: $5s^2\ 5p^6\ 6s^2\ 5d^1\ 4f^0$, Co: $3p^6\ 3d^7\ 4s^2$, and O: $2s^2\ 2p^4$, and we have adopted the values of 2.5 Bohr for La/Bi elements, 1.85 Bohr for cobalt, and 1.6 Bohr for oxygen, as MT radii. The number of plane-wave energy cutoffs $R_{MT}{*}K_{MAX}$ was chosen to be 8.0 for all calculations. A Monkhorst-Pack k-mesh of 12 × 12 × 9 and 10 × 10 × 10 were used for tetragonal and rhombohedric structures, respectively [20]. The convergence of the self-consistent cycles (SCF) was assumed when the energy difference between them was less than 10^{-4} Ry.

3 Results and Discussion

3.1 Magnetic-Phase Stability

Bismuth cobaltite based oxide $BiCoO_3$ crystallize in tetragonal structure with $P4mm$ space group No. 99 (Fig. 1) In order to explore the magneticphase stability, we compare the total energy of $BiCoO_3$ in different magnetic phases relative to the paramagnetic (PM) state. Calculations are done for an artificial nonspin-polarized case, as well as ferromagnetic (FM), AFM-C, antiferromagnetic in three directions (AFM-G), and ferromagnetic abplanes stacked antiferromagnetically along the c axis (AFM-A). The calculated results are shown in Fig. 1. We find that the total energy of the AFM-C phase is the lowest, which is consistent with experimental observations [21, 22] and other theoretical results [23–25].

According to Fig. 1a, we can see that AFM-C ordering is favored, and the superexchange coupling is dominated in ab-plane which confirms the gain energy of AFM-G

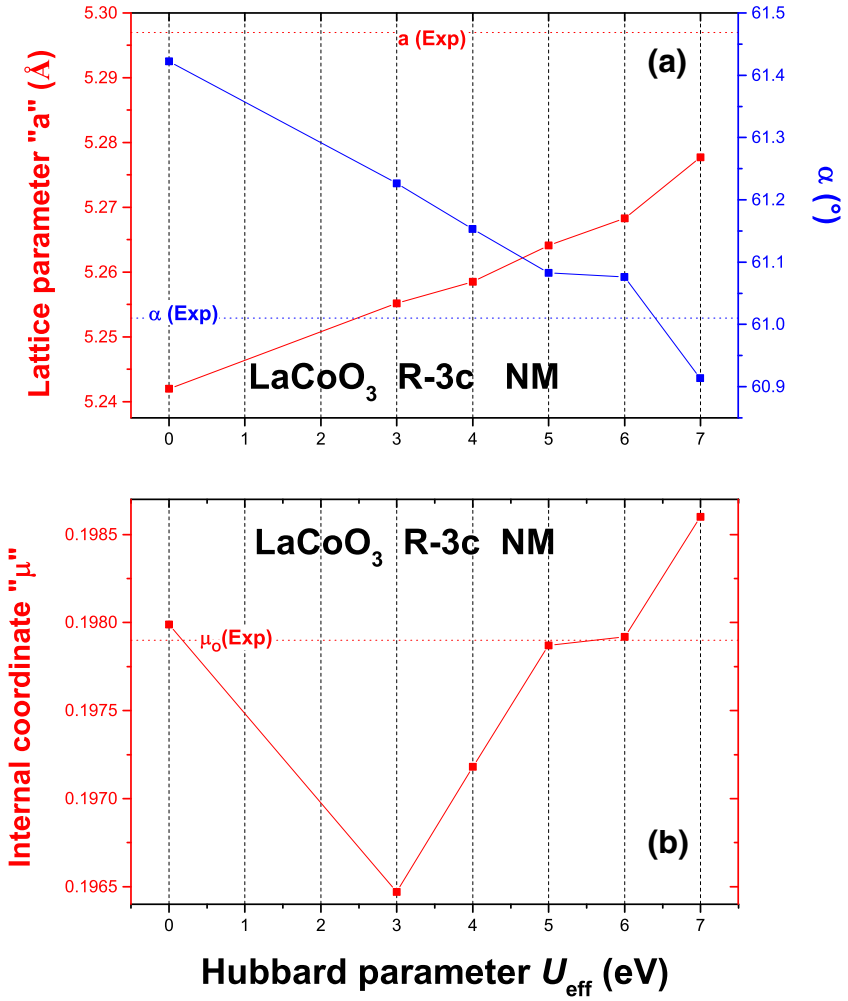

Fig. 5 **a** Variation of a and α versus U_{eff} value for $LaCoO_3$ **b** Variation of internal parameter x versus U_{eff} value for $LaCoO_3$

and AFM-C compared with FM and AFM-A (the *ab*-plane stacked ferromagnetically). The spinordering priority of AFM-C compared with AFM-G is due to the charge transfer between neighboring oxygen atoms This energy gain make AFM-C magnetic structure more favorable compared with AFM-G.

The groundstate determination, lattice parameters, electronic structure, and magnetic properties of $BiCoO_3$ are calculated by employing the LSDA+U schemes, which give the accurate magnetic structure. The value of U does not affect the magnetic structure result.

Next, the magnetic stability of the hypothetical compound tetragonal $LaCoO_3$ was investigated with the selected Hubbard parameter of $BiCoO_3$ tetragonal ($U = 6$ eV) and presented in Fig. 1c. It is clear that the same spin ordering appears in hypothetical $LaCoO_3$ tetragonal, which is due to the similar atomic size of both La and Bi atoms.

The prototypical $LaCoO_3$ has a rhombohedrally distorted pseudo-cubic perovskite structure with space group $R3c$. Compared with the cubic structure, the corner-shared CoO_6 octahedra are tilted and the point symmetry of the central Co ion is reduced from the cubic O_h to the trigonal C_{3i} one. All the Co–O bond lengths $l_{\text{Co-O}}$ are kept the same. The ground state of $LaCoO_3$ is in diamagnetic phase in the LS [26]. To confirm this result, we have done two different calculations of $LaCoO_3$, no spin-polarized calculation and spin-polarized one.

There are three possible configurations of spin in $Co+^3$ ions, the nonmagnetic state is derived from LS and the magnetic state is derived from IS or HS.

To our knowledge, $BiCoO_3$ rhombohedral is a hypothetical compound. Figure 2 shows the nonspin-polarized and spin-polarized states for La/$BiCoO_3$ and it is clear that both materials are nonmagnetic for all values of Hubbard parameter U_{eff} (see Fig. 2a, b). The determination of spin state in this rhombohedral material is an important step to understand the magnetic properties of these compounds. The nonmagnetic state in both compounds explains the LS (S = 0). Since $LaCoO_3$ is a strong correlated material, certainly, the effect of Hubbard parameter U_{eff} is clear. For

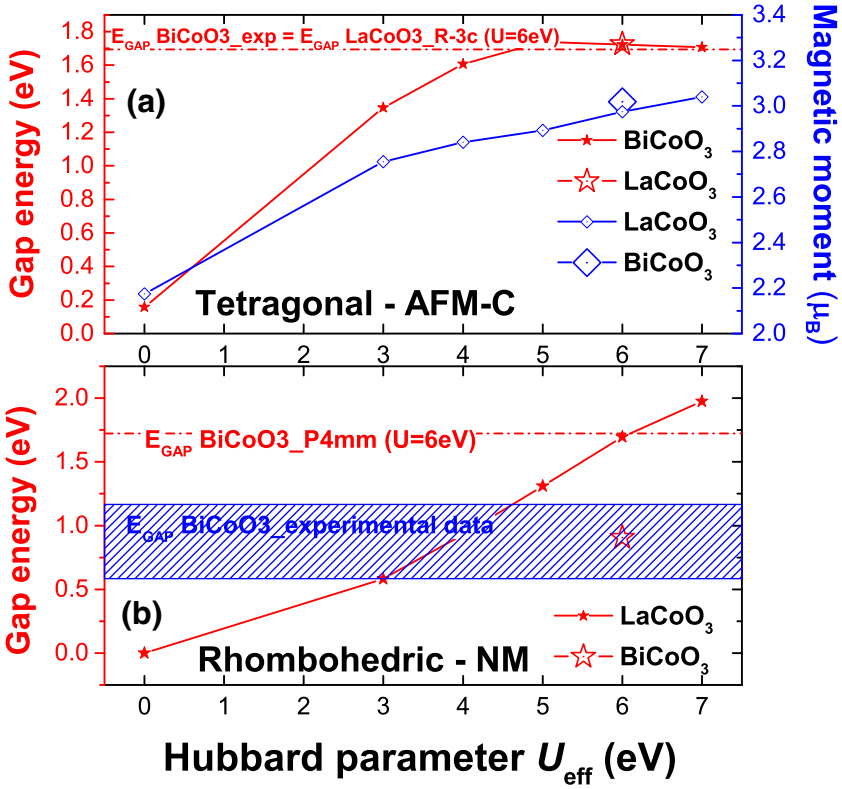

Fig. 6 (**a**) Variation of band gap and spin magnetic moment of $BiCoO_3$ and $LaCoO_3$ in tetragonal structure, with different U_{eff} values comparing with experimental data; (**b**) Variation of band gap of $LaCoO_3$ and $BiCoO_3$ in rhombohedric structure, with different U_{eff} values comparing with experimental data

this, we performed the so-called fixed spin-moment (FSM) calculations [27] within the LSDA+U formalism using Wien2k-code with the variation of U_{eff} (see Fig. 2d). For both cases, the variation energy with total magnetic moment predicts the lowspin state for all U values ($U = 0$ to 6) and beyond $U = 6$ there is change of spin state from LS to IS. So, the total magnetic moment that corresponds to the IS state is around 4 μB which gives to the Co ion a local magnetic moment (MM) of 2 μB. So, we can conclude that the Hubbard parameter U_{eff} affects the result and we should select the best value carefully. Finally we must use U_{eff} value equal or less than 6 eV.

3.2 Structural Properties of $MCoO_3$ (M = Bi, La) Compounds

In this section, we have calculated the total energies of Bi/$LaCoO_3$ materials in tetragonal and rhombohedral structures, with and without Hubbard U parameter application. Calculations were performed using LSDA+U for $U = 0$, 3, 4, 5, 6 and 7. In Fig. 3a–d, we have presented only the results for LSDA+U ($U =$ and 6 eV).

The effect of U effective on the structural stability is clear in $BiCoO_3$ (BCO) than $LaCoO_3$ (LCO). From Fig. 3b, d, it is clear that the LCO adopts a rhombohedric structure which

Table 3 Calculated results of gap size (E_g) and magnetic moment per Co for BCO and LCO materials (values set in italics are in good agreement with experimental data)

	$BiCoO_3$T AFM-C		$LaCoO_3$R NM
	E_g (eV)	Magnetic moment/Co (μ_B)	E_g (eV)
LDA+U, $U = 0$[a]	0.15705	2.17381	–
LDA+U, $U = 3$[a]	1.34708	2.7548	0.58164
LDA+U, $U = 4$[a]	1.608	2.84047	0.9322
LDA+U, $U = 5$[a]	1.7388	2.84047	1.31008
LDA+U, $U = 6$[a]	1.72282	2.97489	1.69486
LDA+U, $U = 7$[a]	1.7067	3.03908	1.97525
LDA+U	2.11 [25]	2.48 [25]	0.7 [30], 2.06 [31]
Unresricted Hartree-Fock	3.31 [32]	3.32 [32]	–
Experiment	1.7 [33]	3.24 [21]	0.9 ± 0.3 [34]

[a]Present calculation

is experimentally confirmed [26] and U parameter does not affect the structural stability. However, the experimental result shows a tetragonal groundstate structure for $BiCoO_3$ [23–25] which does not appear in our LSDA calculation (U = eV) (see Fig. 3a). This failure of LSDA was corrected by application of LSDA+U with a large value of U_{eff}.

Theoretical and experimental values of lattice parameters (a, c/a) and internal parameter z are represented in Table 1.

All past works suggest that $BiCoO_3$ should rather be categorized as a Mott insulator, which requires DFT+U calculation, but unfortunately, the application of U parameter in LSDA increases the volume and tetragonality (c/a). However, this exchange-correlation approximation gives good results in electronic properties. Figure 4a, b and Table 1 show the effect of Hubbard U parameter on lattice parameters and atomic positions of $BiCoO_3$ compound; Fig. 4c shows also the effect of U_{eff} on the volume and c/a of $BiCoO_3$, which confirms that $U_{\text{eff}} = 6$ eV is a best value for giving a good structural parameters of ground state.

We have studied with success the ground state of our systems compared with experimental and theoretical investigations. $BiCoO_3$ adopts a tetragonal structure because the existence of Bi ion and especially *s orbital* in valence states that promotes a shift of cobalt position from his centrosymmetric site (*lone pair* mechanism). However, in $LaCoO_3$, there is no displacement of Co atom and no *lone pair* effect.

We present in Table 2 all structural data of rhombohedral $LaCoO_3$ compound and Fig. 5 shows the Hubbard potential effect on the structural parameters.

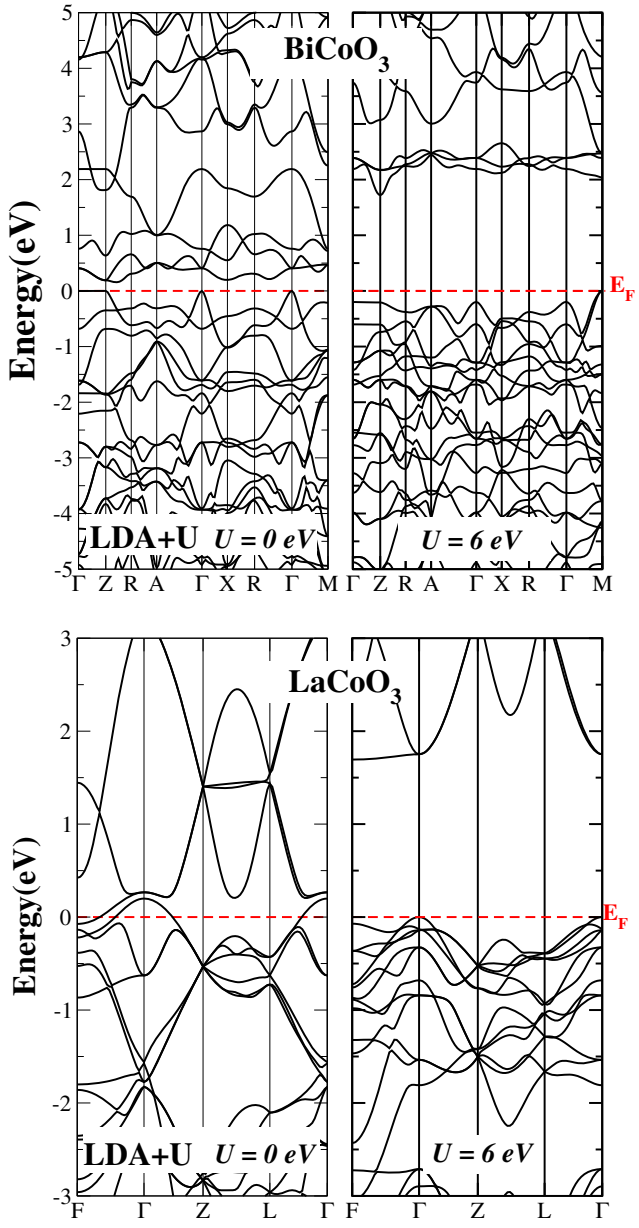

Fig. 7 Band structures of La/$BiCoO_3$ using Ueff = 0 and 6 eV

3.3 Band Structures

First, we will discuss the main features of the Bi/$LaCoO_3$ band structures $E(k)$ and the effect of U parameter in the standard LSDA calculations. Figure 6 shows the band structures $E(k)$ along the high-symmetry lines in an energy range close to the Fermi level of $BiCoO_3$ and $LaCoO_3$, respectively.

There is a clear effect of U_{eff} on band structures in both compounds through an important correction of states from metallic to insulator nature.

Table 3 presents a different values of gap energies for Bi/$LaCoO_3$ with LSDA+U ($U = -7$ eV) compared with experimental and theoretical data. Our results shown in Fig. 6 confirm the good choice of a large U_{eff} ($U = 6$ eV).

For both compounds, an indirect band gap is localized (the valence-band maximum at M and the conduction-band minimum at Z for BCO, the valence-band maximum at Γ and the conduction-band minimum at F for LCO). Using LAPW-LSDA+U, we have predicted the band gap and magnetic moment with a good accuracy. Since the ionic radius of La and Bi are nearly equal, and cobalt environment are the same in both structures, we have found equivalent band gap energies in both materials.

3.4 Density of States and Magnetic Moment

Total and partial DOS of $BiCoO_3$ and $LaCoO_3$ in the AFM-C tetragonal structure obtained by LSDA+U (U = 6 eV) are shown in Figs. 7 and 8. TDOS of LCO presents a metallic character using LSDA and a semiconductor character by LSDA+U. For BCO, the insulator character is present, and the band gap energy increases with the application of U_{eff}. From Fig. 7, we notice that there are unoccupied Co 3d states (hybridized with O 2p orbital)

extending from 2 to 2.8 eV and the width of this unoccupied band is about 0.8 eV. According to partial DOS of Bi, Co, and O, there are occurrences of strong hybridization effects O $2p$-Co $3d$ and Bi $(6s, 6p)$-O $2p$ states. It is accepted generally that the ferroelectricphase transition arises from a delicate balance between long-range Coulomb forces (which favors the ferroelectric state) and short-range repulsions (which favors the nonpolar structure) [25]. The hybridization between Co $3d$ and O $2p$ leads to the charge transfer from O to Co; thus, O (2.535) and Co (4.5884↑ and 1.6357↓) are not fully ionized. The covalent Co–O bonds which extended from −7.5 eV to E_F, will weaken the short-range repulsions and reduce the total energy, which is favorable for the ferroelectricphase transition. Moreover, the Bi s state is fully occupied and acts as a lone pair state causing the off centering of Co ion [25]. The covalence of Bi–O (− 10 to − 9 eV) causes a partially charge transfer from O to both Bi, which reduces the total energy and enhances the stability of the ferroelectric structure of $BiCoO_3$. On the other hand, the hybridizations of Co–O cause the large decrease of spin magnetic moments of Co ions 2.97 μB in comparison with the d^6 configuration 4 μB. Moreover, Fig. 7 shows a hybridization between Co d_{xz}, d_{yz}, and O p_z, which is missing between d_{xy} and p_z. This remark confirms the localization character of d_{xy} orbital. From Fig. 7, we can observe the occupancy of Co d orbital as follows: d_{xy} ↑, d_{xz} ↑, d_{yz} ↑, d_z^2 ↑, and $d_{x^2-y^2}$ ↑↓. This result confirms that the t_{2g}orbital is higher than $e_g$orbital,

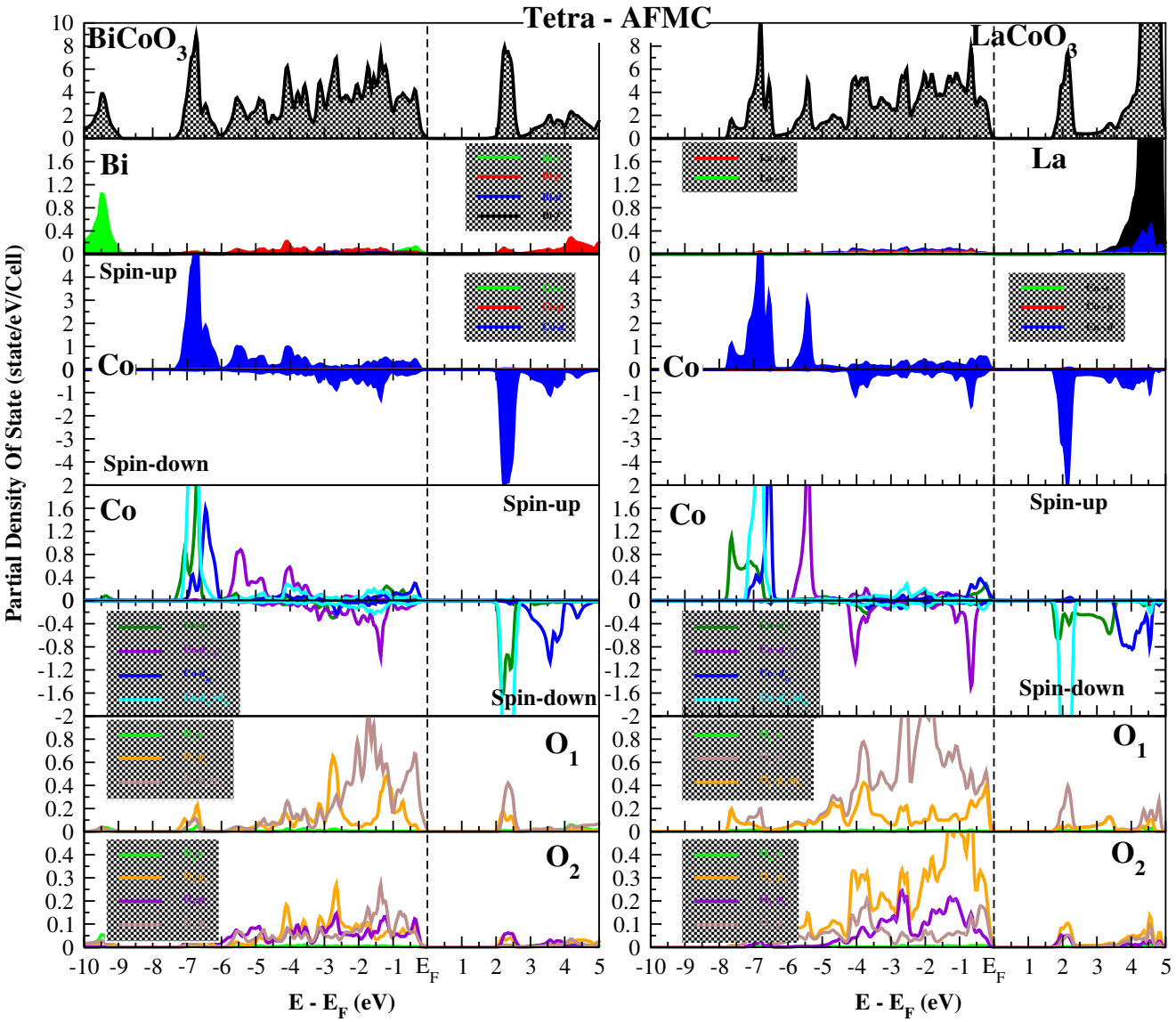

Fig. 8 Total and partial DOS of $BiCoO_3$ and $LaCoO_3$ in the NM rhombohedral structure obtained by LSDA+U ($U = 6$ eV)

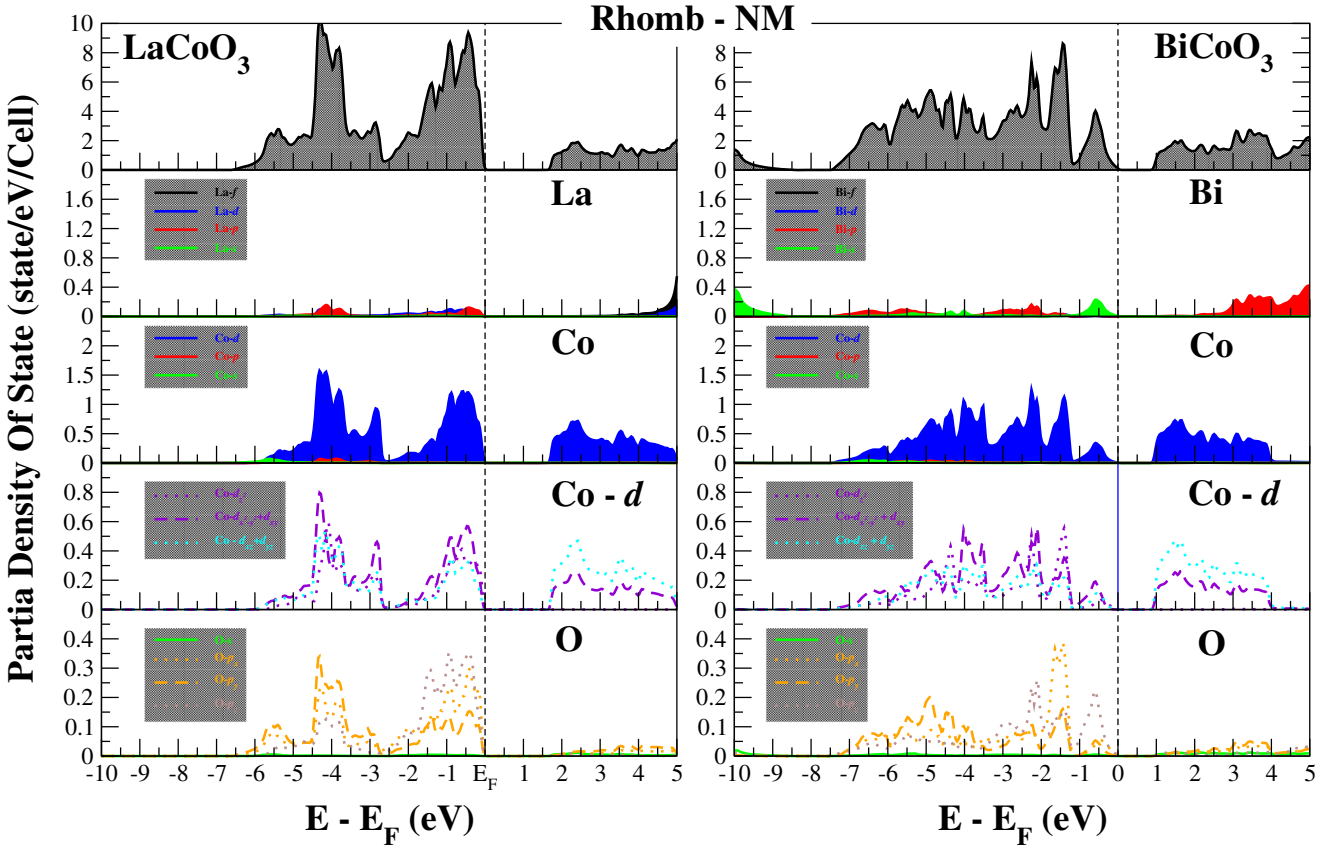

Fig. 8 (continued)

where the down electron prefers $e_g$orbital. The last result shows the HS state in BCO-T with magnetic moment of 2.97 μB reduced by Co–O covalent bond.

The crystal field in BCO is present due to the octahedral environment of Co ion. From our BCO-DOS, there is a splitting of partial *d*-orbitals of cobalt due to the Jahn-Teller effect that arises because regular octahedra deformed into a tetragonal distortion to lift the cubic symmetry. Nevertheless, in this type of transition metal oxides, the C-type or G-type antiferromagnetic spin state results from the superexchange mechanism. In the case of $BiCoO_3$, the C-type AFM is favored because of the existence of charge transfer between nearest-neighbor oxygen, where the transport properties follow Co–O–O–Co path. O–O charge transfer reduces the total energy of system and makes the AFM-C state more stable than AFM-G. In the hypothetical tetragonal AFM-C $LaCoO_3$, we remark the same hybridization and covalent bond between Co and O atoms (see Fig. 7). However, the absence of hybridization between La *s*and *p*orbitals and O *p*orbital makes the lone pair effect absent, which disadvantage the Co displacement and ferroelectric phase.

Figure 8 shows the calculated density of states in nonmagnetic configuration (LS: $t_{2g}^6 e_g$) for the rhombohedric $LaCoO_3$, where t_{2g} is fully occupied with triply degenerated d_{xy}, d_{xz}, and d_{yz} orbitals (same energies in DOS). The valence band is formed by a mixture of Co states and O 2*p* orbitals while the doubly degenerate $d_{x^2-y^2}$ and d_{z^2} orbitals, which represent the e_g manifold, form the conduction band and the valence band, which is characterized by two peaks at − 0.5 and − 4.5 eV below the Fermi energy, representing strong hybridization of electrons of O and Co atoms with some small contribution from La atom. In the hypothetical rhombohedric $BiCoO_3$, there is a small hybridization between Bi *s* and O *p* orbitals, which can cause a displacement of Co atom and consequently the tilt of the octahedral.

4 Conclusion

Using the first-principle DFT method and LSDA+*U* calculations, we have performed a detailed investigation on the structural and magnetic ground states of strongly

correlated perovskites, $BiCoO_3$ and $LaCoO_3$. We have found a critical value of $U_{\text{eff}} = 6$ eV that induces a spinstate transition in the bulk rhombohedral $LaCoO_3$ structure. The variation of U induces a structural transition from rhombohedric to tetragonal in bulk $BiCoO_3$. Our result shows that the correct tetragonal AFM-C structure is stable for U_{eff} values more than 4.0 eV. According to these two critical values of U_{eff} (between 4.0 and 6.0 eV), $BiCoO_3$ adopts the antiferromagnetic state with C-type spin ordering and $LaCoO_3$ was found nonmagnetic with lowspin configuration of Co d electrons. Structural parameters of $BiCoO_3$ compound in tetragonal-AFM-C structure and of $LaCoO_3$ in rhombohedric-NM structure using $U_{\text{eff}} = 6$ eV, are found in good agreement with other experimental and theoretical works.

The band structures of these compounds confirm the insulator character for both materials with a large band gap. We have also examined the density of states for the synthesized T-$BiCoO_3$-AFM-C and R-$LaCoO_3$-NM compounds and the hypothetical T-$LaCoO_3$-AFM-C and R-$BiCoO_3$-NM compounds. There are occurrences of strong hybridization effects O $2p$-Co $3d$ and Bi ($6s$, $6p$)-O $2p$ states. The covalent Co–O bonds will weaken the short-range repulsions and reduces the total energy, which is favorable for the ferroelectricphase transition. Moreover, the Bi s state is fully occupied and acts as a lone pair state causing the off centering of Co ion. On the other hand, the hybridizations of Co–O cause the large decrease of spin magnetic moments of Co ions at 2.97 μB in comparison with the d^6 configuration 4 μB. Our results show the HS state in BCO-T with a magnetic moment of 2.97 μB reduced by Co–O covalent bond. There is a splitting of partial d-orbitals of cobalt due to the Jahn-Teller effect that arises by the octahedral deformation to lift the cubic symmetry. From our calculations, there are clear similarities between BCO-R and LCO-R. However, the absence of hybridization between La s and p orbitals and O p orbital does not induce the lone pair effect and consequently the ferroelectric phase is not favored.

References

1. Hill, N.A.: J. Phys. Chem. **104**, 6694 (2000)
2. Scott, J.F.: Nat. Mat. **6**, 256 (2007)
3. Picozzi, S., Yamauchi, K., Sergienho, I., Sanyal, B., Dagatoo, E.: J. Phys. Condens. Matter. **20**, 434208 (2008)
4. Kanungo, S., Saha-Dasgupta, T.: Phys. Rev. B **83**, 104104 (2011)
5. Belik, A.A., Azuma, M., Saito, T., Shimakawa, Y., Takano, M.: Chem. Mater. **17**, 269 (2005)
6. Neaton, J.B., Ederer, C., Waghmare, U.V., Spaldin, N.A., Rabe, K.M.: Phys. Rev. B **71**, 014113 (2005)
7. Nelmes, R.J., Kuhs, W.F.: Solid State Commun. **54**, 721 (1985)
8. Sudayama, T., Wakisaka, Y., Mizokawa, T., Wadati, H., Sawatzky, G.A., Hawthorn, D.G., Regier, T.Z., Oka, K., Azuma, M., Shimakawa, Y.: Phys. Rev. B **83**, 235105 (2011)
9. Belik, A.A., Iikubo, S., Kodama, K., Igawa, N., Shamoto, S.I., Niitaka, S., Azuma, M., Shimakawa, Y., Takano, M., Izumi, F., Takayama-Muromachi, E.: Chem. Mater. **18**, 798 (2006)
10. Ravindran, P., Vidya, R., Eriksson, O., Fjellvag, H.: Adv. Mater. **20**, 1353 (2008)
11. Tokura, Y., Okimoto, Y., Yamaguchi, S., Taniguchi, H., Kimura, T., Takagi, H.: Phys. Rev. B **58**, R1699 (1998)
12. Radaelli, P.G., Cheong, S.-W.: Phys. Rev. B **66**, 094408 (2002)
13. Jia, T., Wu, H., Zhang, G., Zhang, X., Guo, Y., Zeng, Z., Lin, H.-Q.: Phys. Rev. B **83**, 174433 (2011)
14. Kan, D., Palova, L., Anbusathaiah, V., Cheng, C.J., Fujino, S., Nagarajan, V., Rabe, K.M., Takeuchi, I.: Adv. Funct. Mater. **20**, 1108 (2010)
15. Blaha, P., Schwarz, K., Madsen, G.K.H., Kvasnicka, D., Luitz, J.: WIEN2K, an augmented plane wave plus local orbitals program for calculating crystal properties. Vienna University of Technology, Vienna (2001)
16. Sjöstedt, E., Nordstrom, L., Singh, D.J.: Solid State Commun. **114**, 15 (2000)
17. Perdew, J.P., Wang, Y.: Phys. Rev. B **45**, 13244 (1992)
18. Zaanen, V.I., Anisimov, J., Andersen, O.K.: Phys. Rev. B **44**, 943 (1991)
19. Murnaghan, F.D.: Proc. Natl. Acad. Sci. USA **30**, 5390 (1944)
20. Monkhorst, H.J., Pack, J.D.: Phys. Rev. B **13**, 5188 (1976)
21. Belik, A.A., Iikubo, S., Kodama, K., Igawa, N., Shamoto, S.I., Niitaka, S., Azuma, M., Shimakawa, Y., Takano, M., Izumi, F., Takayama-Muromachi, E.: Chem. Mater. **18**, 798 (2006)
22. Sudayama, T., Wakisaka, Y., Oka, K., Azuma, M., Shimakawa, Y., Wadati, H., Sawatzky, G.A., Hawthorn, D.G., Regier, T.Z., Mizokawa, T.: Canadian Light Source, 128 (2009)
23. Ravindran, P., Vidya, R., Eriksson, O., Fjellvag, H.: Adv. Mater. **20**, 1353 (2008)
24. Uratani, Y., Shishidou, T., Ishii, F., Oguchi, T.: Jpn. J. Appl. Phys. **44**, 7130 (2005)
25. Cai, M.-Q., Liu, J.-C., Yang, G.-W., Cao, Y.-L., Tan, X., Chen, X.-Y., Wang, Y.-G., Wang, L.-L., Hu, W.-Y.: J. Chem. Phys. **126**, 154708 (2007)
26. Raccah, P.M., Goodenou, J.B.: Phys. Rev. **155**, 932 (1967)
27. Schwarz, K., Mohn, P.: J. Phys. F **14**, L129 (1984)
28. Mukhopadhyay, S., Finnis, M.W., Harrison, N.M.: Phys. Rev. B **87**, 125132 (2013)
29. Hsu, H., Umemoto, K., Cococcioni, M., Wentzcovitch, R.: Phys. Rev. B **79**, 125124 (2009)
30. Nekrasov, I.A., Streltsov, S.V., Korotin, M.A., Anisimov, V.I.: Phys. Rev. B **68**, 235113 (2003)
31. Korotin, M.A., Ezhov, S.Yu., Solovyev, I.V., Anisimov, V.I., Khomskii, D.I., Sawatzky, G.A.: Phys. Rev. B **54**, 5309 (1996)
32. Sudayama, T., Wakisaka, Y., Mizokawa, T., Wadati, H., Sawatzky, G.A., Hawthorn, D.G., Regier, T.Z., Oka, K., Azuma, M., Shimakawa, Y.: Phys. Rev. B **83**, 235105 (2011)
33. McLeod, J.A., Pchelkina, Z.V., Finkelstein, L.D., Kurmaev, E.Z., Wilks, R.G., Moewes, A., Solovyev, I.V., Belik, A.A., Takayama-Muromachi, E.: Phys. Rev. B **81**, 144103 (2010)
34. Abbate, M., Fuggle, J.C., Fujimori, A., Tjeng, L.H., Chen, C.T., Potze, R., Sawatzky, G.A., Eisaki, H., Uchida, S.: Phys. Rev. B **47**, 16124 (1993)